Journal of Alloys and Compounds 488 (2009) 314–319

Contents lists available at ScienceDirect

Journal of Alloys and Compounds

journal homepage: www.elsevier.com/locate/jallcom

# Preparation, characterization of P-doped $TiO_2$ nanoparticles and their excellent photocatalystic properties under the solar light irradiation

Yingying Lv[a,b], Leshu Yu[a,c,*], Heyong Huang[b], Hailong Liu[b], Yuying Feng[b,**]

[a] Department of Chemistry, Shangrao Normal University, Shangrao 334001, China
[b] Analysis and Testing Center, Department of Chemistry and Environmental Science, Nanjing Normal University, Nanjing 210097, China
[c] Key Laboratory of Mesoscopic Chemistry of MOE and School of Chemistry and Chemical Engineering, Nanjing University, Nanjing 210093, China

ARTICLE INFO

*Article history:*
Received 12 August 2009
Received in revised form 16 August 2009
Accepted 17 August 2009
Available online 31 August 2009

*Keywords:*
Oxide materials
Sol–gel processes
Phase transitions
Radiation effects
Optical properties

ABSTRACT

Numerous publications have been reported about the doped $TiO_2$ to extend the photoactive wavelength region to visible light for the enhanced photocatalystic properties under artificial visible light irradiation in recent 20 years. Nevertheless except the commercial Degussa P25, the reports about the photocatalysts under the solar light irradiation are very few. Fully utilizing 4% UV light in solar light may be a preferential selection due to its endless energy, free of charge and the faster degradation rate from the UV light than from the visible light. In this study, P-doped anatase $TiO_2$ nanoparticles were conveniently prepared via a conventional sol–gel route. Due to the reconstructed favorable surface structure with the incorporated P–O–Ti bonds and the larger surface area, the P-doped $TiO_2$ nanoparticles exhibited an enhanced photocatalytic activity for the degradation of rhodamine B (RhB) as compared with Degussa P25 and the undoped or N, S-codoped $TiO_2$ under solar light irradiation. Especially, degradation efficiency of RhB over P-doped under solar light is only a little lower than that under UV light in the same irradiation time, suggesting that such constructed photocatalyst could fully utilize solar light and meet the requirement for practical applications. Furthermore some factors including calcination temperature of photocatalyst, initial concentration of RhB, reuse of the photocatalyst, catalyst dosage and P doping contents were also systematically investigated to evaluate the P-doped $TiO_2$ photocatalytic degradation efficiency under the solar light irradiation. This excellent performance endows the as-prepared P-doped anatase photocatalysts potential in purifying wastewater.



## 1. Introduction

Environmental pollution and destruction gained central focus on a global scale in today's society; thereinto wastewater derived from different chemical industries has high concentration of large organic molecules which are extremely toxic, carcinogenic and refractory in nature, and is arousing increased concern. Certainly using solar light is an optimal way to treat this wastewater problem due to its endless energy and free of charge. Unfortunately, most large organic molecules cannot be effectively decomposed into nontoxic small molecules under long-time solar light irradiation. Hence some effective catalysts have to be a need for the degradation of pollutants. In recent years, there has been an extensive interest in the use of semiconductors as photocatalysts to initiate photocatalytic reactions at their interfaces [1]. Among them, anatase phase titanium dioxide ($TiO_2$) based nanomaterials have been extensively studied as the most promising environment protective photocatalyst because of its nontoxicity, low cost, good chemical stability and high catalytic activity, and Degussa P25 has been seen as the most extensively used commercial photocatalysts hitherto [2–4]. Due to its wide band gap of 3.2 eV, pure $TiO_2$ cannot make use of the visible light in solar. Therefore great efforts were made to dope various metal or nonmetal elements into titania to extend the photoactive wavelength region to visible light and the resulted photocatalysts owned enhanced photocatalystic properties under artificial visible light irradiation, which require substantial electrical power input and cannot meet the requirement for practical applications [5–15]. As far as we know, those doped titania showed inferior photocatalystic effect to the common Degussa P25 under the solar light irradiation-optimal light source [16,17]. In our group similar works were also conducted and the acquired N, Cu-codoped or N, S-codoped titania showed weak photocatalystic effect as a comparison with Degussa P25 under sunlight irradiation [18,19]. Furthermore, except the commercial Degussa P25, the reports about the photocatalysts fitting under the solar

* Corresponding author at: Department of Chemistry, Shangrao Normal University, Hankou Road 22#, Shangrao 334001, China. Tel.: +86 25 83685303; fax: +86 25 83686251.
** Corresponding author. Tel.: +86 25 83685303; fax: +86 25 83686251.
*E-mail addresses:* yuleshu2008@126.com (L. Yu), yyfeng3@163.com (Y. Feng).

0925-8388/$ – see front matter © 2009 Elsevier B.V. All rights reserved.
doi:10.1016/j.jallcom.2009.08.116

light irradiation are very few [20]. These experiential results suggested that under the solar light irradiation, merely decreasing the band gap of $TiO_2$ to extend the photoactive wavelength region to visible light through doping elements into titania is not an ideal route to enhance the photocatalystic effect. Hence developing a good photocatalyst superior to common used Degussa P25 under the solar light irradiation would be an interesting topic.

Since finicky focus on the full utilization of visible light in solar light resulted in the relative less effort on the full utilization of 4% UV light in solar light. Actually, we must realize that: we cannot change the fact that only 4% UV light does exist in solar light. Therefore fully utilizing 4% UV light in solar light may be a preferential selection due to the faster degradation rate from the UV light than from the visible light. Hence increasing the absorption in the UV range for fully utilizing 4% UV light in solar light would be a better method than finicky focusing on the full utilization of visible light in solar light. Very recently we noticed that phosphorus species in titania have attracted increased interest [21–29], and the as-prepared P-doped $TiO_2$ powders owned more superior properties including photocatalytic activity and high-temperature stability over Degussa P25 under UV irradiation. However the photocatalytic activity of P-doped $TiO_2$ has not been examined under the solar light irradiation. In this study, P-doped anatase $TiO_2$ nanoparticles were conveniently prepared via a conventional sol–gel route. Due to the stronger absorption in the UV range and the larger surface area, the as-prepared P-doped $TiO_2$ exhibited an enhanced photocatalytic activity for the degradation of rhodamine B as compared with the undoped, N, S-codoped $TiO_2$ and Degussa P25 under solar light irradiation, indicating that the as-prepared P-doped anatase photocatalysts have better catalytic activity and potential applications in purifying wastewater.

## 2. Experimental

### 2.1. Preparation of P-doped $TiO_2$ nanoparticles

P-doped $TiO_2$ nanoparticles were synthesized by sol–gel method similar to our previous work [19]. Herein, tetrabutyl titanate ($C_{16}H_{36}O_4Ti$) was used as a precursor, the analytical grade phosphoric acid ($H_3PO_4$) as a phosphorus source. The typical process could be described as follows. The molar ratio of phosphoric acid and tetrabutyl titanate is 0.044. (1) 30 μL of phosphoric acid, 10 mL of hydrochloric acid (pH = 2) and 20 mL of ethanol was mixed to form a homogeneous solution. (2) 4 mL of tetrabutyl titanate and 4 mL of acetic acid were dissolved in 20 mL of ethanol. (3) A stable and transparent colloid solution can be obtained by dropping the solution prepared in step 1 into the step 2 mixtures after constant stirring for 3 h. (4) Then the colloid was dried at 120 °C. (5) The obtained powder was calcined in a muffle at various temperatures for 3 h to obtain different P-doped $TiO_2$ samples. For a comparison, the undoped and N, S-codoped $TiO_2$ samples were also prepared with a similar procedure [19].

### 2.2. Characterization technique

Ultraviolet–visible (UV–Vis) diffuse reflectance spectra were performed using VARIAN Cary-5000 UV/Vis/NIR spectrophotometer. $BaSO_4$ was used as a reflectance standard sample. X-ray diffraction (XRD) measurements utilized a Philips X'pert Pro X-ray diffractometer with Cu Kα radiation of 1.5418 Å. X-ray photoelectron spectra (XPS) were acquired with a VG ESCALAB MKII X-ray photoelectron spectrophotometer. The Fourier transform infrared (FTIR) spectra of the samples mixed with KBr were recorded on a Nicolet Magna 560 FTIR spectrometer at a resolution of 2 $cm^{-1}$. The Brunauer–Emmett–Teller (BET) surface area is determined by Micromeritics ASAP 2020 nitrogen adsorption equipment at liquid nitrogen temperature.

### 2.3. Study of photocatalytic activity

The photocatalytic activity of the P-doped $TiO_2$ samples was evaluated by the photodegradation of rhodamine B (RhB) aqueous solution with an initial concentration of 12 mg/L. Herein solar light was used as the preferential light source and a 500 W mercury lamp was used sometimes for UV light source. The sunlight experiments were carried out between 10.00 a.m. and 14.00 p.m. during the days of November (winter season) at Nanjing City. Unless otherwise noted, 5 mg of catalyst powder was added into 25 mL of above RhB solution in a quartz tube, corresponding to a catalyst dosage of 0.2 g/L. Prior to irradiation, the suspensions were magnetically stirred in dark for 30 min to ensure the establishment of an adsorption/desorption equilibrium. At given time intervals, about 4 mL aliquots were sampled, centrifuged. The above clear solution was analyzed by recording variations in the absorption in UV–Vis spectra of RhB. According to the standard curve between concentration and absorption, the value of $(1 - C/C_0)$ was calculated, denoted as the degradation ratio.

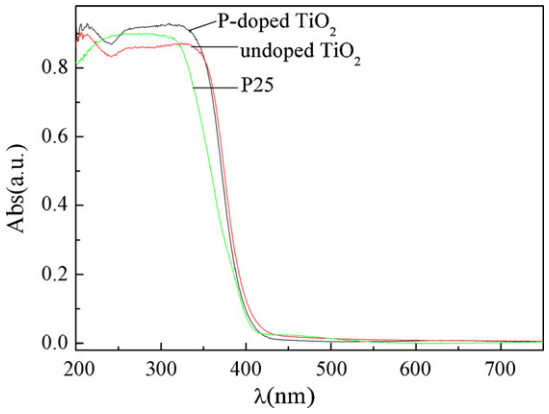


**Fig. 1.** UV–Vis absorption spectra of the as-prepared $TiO_2$ powders and Degussa P25.

## 3. Results and discussion

### 3.1. UV–Vis diffuse reflectance spectra of the photocatalysts

The UV–Vis diffuse reflectance spectra of the photocatalysts are shown in Fig. 1. By a simple calculation, the band gaps of the P-doped, undoped $TiO_2$ and P25 are 3.02, 3.00 and 3.05 eV, respectively, indicating that the P-doped sample did not shifted to the longer wavelength region and the band gap is still very big. This case is consistent with the computation results in P-doped anatase $TiO_2$ [30]. No redshift of the P-doped titania implied that the as-prepared sample would not utilize fully the visible light in sunlight. But the P-doped nanoparticles have a strongest absorption in the UV range than the undoped $TiO_2$ and P25. So the prepared P-doped sample can utilize fully the most UV light in sunlight than the other two, suggesting that the P-doped $TiO_2$ would be an ideal photocatalyst under the solar light irradiation.

### 3.2. Structural analysis of the photocatalysts

Fig. 2 shows the XRD patterns of the P-doped and undoped powders annealed at different temperatures. From Fig. 2a, it is clear that the P-doped sample calcined below 900 °C reveals anatase $TiO_2$ and that a new species corresponding to the cubic $TiP_2O_7$ calcined at 900 °C was observed. The thermal stability of the P-doped samples was further supported by Raman spectroscopy (Fig. S1). However in Fig. 2c, the undoped $TiO_2$ does not stand up with the high-temperature annealing and begins to show rutile phase at 800 °C. Additionally, it is worth noting that the peaks corresponding to the (1 0 1) plane for P-doped and undoped anatase $TiO_2$ could not be well accordant and are shown in Fig. 2(b) and (d). For the P-doped sample, when annealed below 900 °C, the (1 0 1) plane is located at 25.40°, but when annealed at 900 °C, the (1 0 1) plane of anatase shifted to lower angle of 25.25° while cubic $TiP_2O_7$ is separated out from the anatase matrix. However in the undoped sample anatase $TiO_2$, this case does not happened, its (1 0 1) plane peak does not vary with the annealing temperature. Hence from the shift of (1 0 1) plane of P-doped sample, it is very possibly implied that the P element should be doped into the crystal lattice of anatase. Since the radii of P ion (0.38 Å) is smaller than that of Ti ion (0.67 Å) [29], along with the separation of P ion, the (1 0 1) plane of anatase was shifted to lower diffraction angle. If the radii of dopant atom are close to that of O atom or Ti atom, the diffraction peak of (1 0 1)

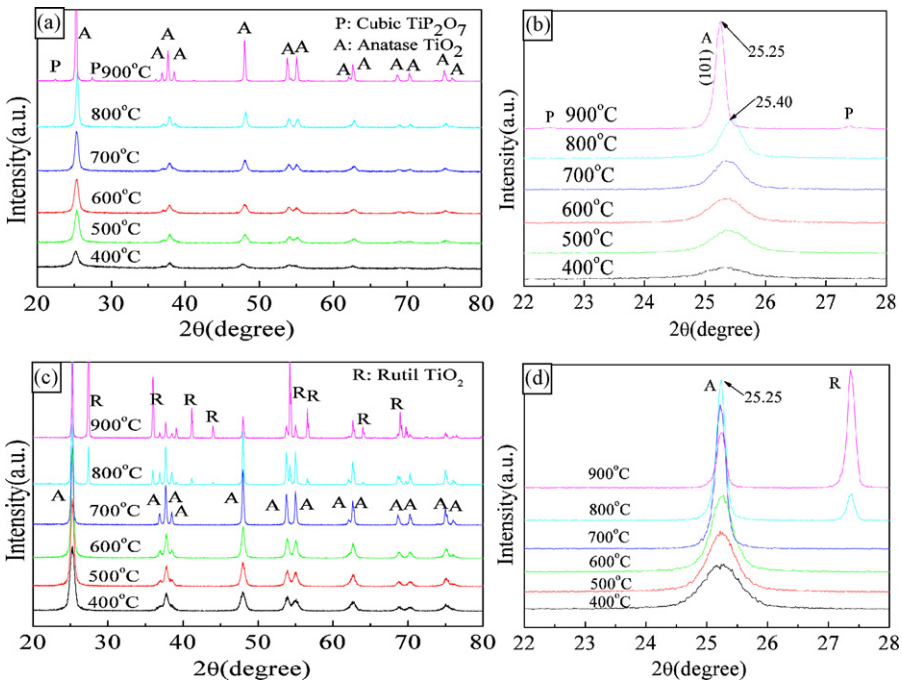


**Fig. 2.** X-ray diffraction patterns of P-doped (a) and undoped titania (c) annealed at different temperatures. The right patterns (b and d) are the corresponding local enlargements from the whole XRD patterns.

plane of the F-doped anatase samples does not shift under the high-temperature anneal [31].

Fig. 2 also shows that the (1 0 1) planes of P-doped or undoped samples are turned more and more aculeate with the annealing temperature increasing, indicating the higher crystalline degree and the larger nanoparticles for the samples. The typical crystallite sizes of nanoparticles for the annealing P-doped sample at 500 °C is 12.1 nm via calculated from the Scherrer equation [32]. Transmission electron microscopy image (TEM) (Fig. S2) indicates that the mean particle sizes of these samples are about 12 nm in diameter, which is in fairly good agreement with the data calculated from XRD. From Fig. S2, mesopores are clearly observed into the nanoparticles.

### 3.3. XPS and FTIR analysis

X-ray photoelectron spectroscopy (XPS) measurements could reveal the chemical states of doped samples, which are pivotal to the optical property, band gap, and photocatalytic activity of nonmetal-doped $TiO_2$. Fig. 3 shows XPS curves of $P_{2p}$, $Ti_{2p}$ and $O_{1s}$ taken on the surface of P-doped sample annealed at 500 °C, and from the measurement the P content is about 1.57 atom% though the molar ratio of phosphoric acid and tetrabutyl titanate is 0.044. In Fig. 3a, there is only one peak at 133.2 eV, indicating that P ions are in the pentavalent-oxidation state ($P^{5+}$). Hence Ti atoms are unlikely to bond P atoms to form Ti–P bonds in the P-doped $TiO_2$ since the characteristic peak of P in Ti–P at 129 eV has not been observed. Thus, it is seemed that the $P^{5+}$ replaced a part of $Ti^{4+}$ in the crystal lattice of $TiO_2$, which resulted in the charge imbalance and decreased the recombination rate of photogenerated electrons and holes [33]. Seen from Fig. 3c, $O_{1s}$ region of P-doped $TiO_2$ nanoparticles can be fitted by three peaks, including Ti–O bonds, P–O bonds and C–O bonds, respectively, which further support the view of the presence of Ti–O–P bonds. Similar to the cases of the surface-terminating Ti–O–B–N structures in N, B-codoped anatase, herein the Ti–O–P surface structures in P-doped anatase may act as reactive sites for promoting the surface separation of photoinduced charge carriers [34–36].

FTIR spectra of the P-doped, undoped $TiO_2$ annealed at 500 °C and Degussa P25 samples are shown in Fig. 4. The broad peak at 3404 $cm^{-1}$ and the peak at 1632 $cm^{-1}$ of the P-doped $TiO_2$ could be indexed to OH stretching and bending vibrations, respectively, and became stronger than those of undoped $TiO_2$ and P25. This case suggests that more surface-adsorbed water and hydroxyl groups

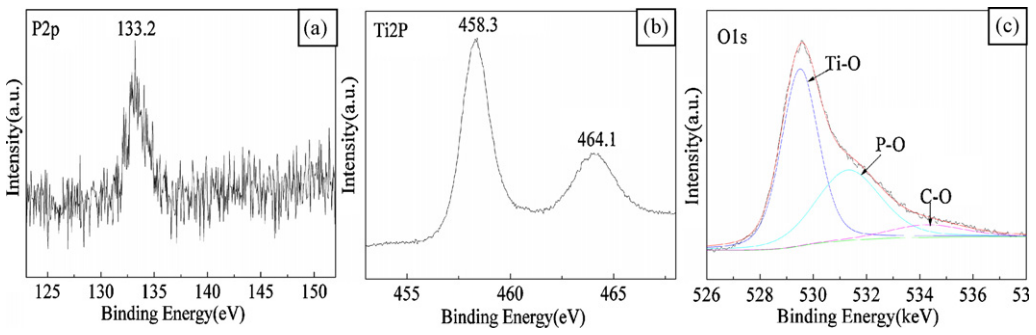


**Fig. 3.** X-ray photoelectron spectra (XPS) spectra for the P-doped $TiO_2$ sample in the binding energy ranges of (a) $P_{2p}$, (b) $Ti_{2p}$, and (c) $O_{1s}$.

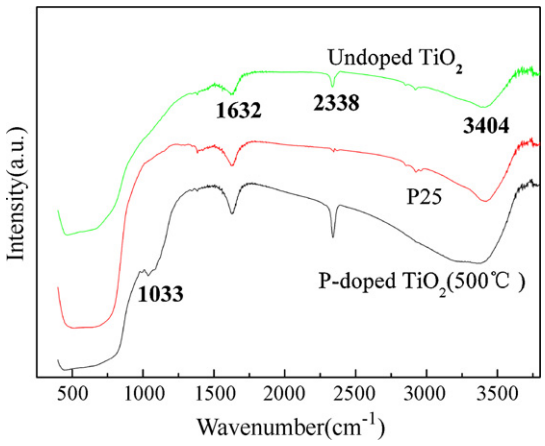


**Fig. 4.** The Fourier transform infrared (FTIR) spectra of the P-doped, undoped $TiO_2$ annealed at 500 °C and Degussa P25 samples.

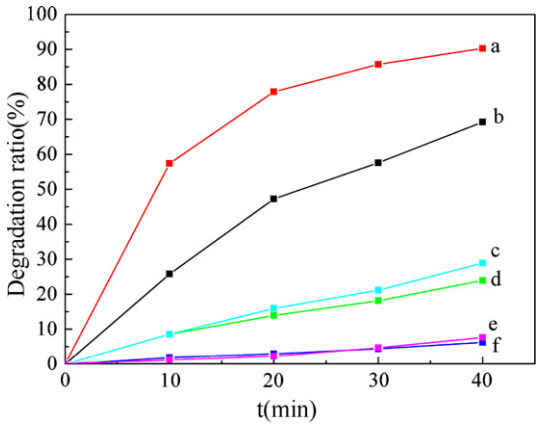


**Fig. 5.** Degradation ratio of rhodamine B (RhB) on (a) P-doped $TiO_2$, (b) Degussa P25, (c) N, S-codoped, (d) undoped $TiO_2$, (e) RhB without the presence of any photocatalyst under solar irradiation for 40 min and (f) photosensitization degradation of RhB in the presence of P-doped $TiO_2$ but without the solar irradiation.

exist in the P-doped sample than in the undoped samples and P25, which are quite helpful for the surface photocatalytic reaction onto the P-doped $TiO_2$ [1,3,37–39]. In addition, an absorption peak at 1033 $cm^{-1}$ is observed in the IR spectra of P-doped $TiO_2$ but absent for undoped $TiO_2$ and P25 samples. This characteristic frequency is resulted from the doped P atoms which exist in the form of Ti–O–P, with P replacing part of $Ti^{4+}$ in the titania lattice [29]. Based on the analysis of XPS and IR, it can be inferred that the P element has been successfully doped into $TiO_2$, which are well accordance with the results of XRD pattern.

### 3.4. BET analysis

The BET specific surface areas of the P-doped, undoped $TiO_2$ and P25 are summarized in Table 1. With the same calcination temperature, the surface area of P-doped titania was significantly larger than that of the undoped one and 2.5 times of that of P25. Hence P doping into $TiO_2$ helps to markedly increase the surface area. The evolution of pore distribution of the three photocatalysts above is similar to the BET surface areas (Fig. S3). In addition, for P-doped samples annealed at different temperatures, their surface area decreased with increasing calcinations temperature (Table S1) due to the high-temperature sintering. Anyway, herein the as-prepared P-doped titania annealed at 500 °C with large surface area would be an ideal photochemical reaction sites.

### 3.5. Evaluation of photocatalytic activity of P-doped $TiO_2$

To explore the photocatalytic activity of P-doped $TiO_2$ (500 °C), the degradation of RhB by solar light was investigated. The photocatalytic degradation capability of the undoped and N, S-codoped $TiO_2$ (500 °C) [19] and Degussa P25 are also measured as a reference to that of the P-doped sample. Fig. 5 shows a comparison of the degradation ratio of RhB on different catalysts calcined at 500 °C under solar light irradiation. The RhB itself degradation without a catalyst and the photosensitization degradation of RhB in the presence of photocatalysts were also investigated. As can be seen from Fig. 5, the self-photosensitized process of RhB can be nearly negligible as compared with the photocatalytic process, showing the RhB degradation have two prerequisites: sunlight and photocatalyst. It is clear that the P-doped $TiO_2$ (500 °C) shows the highest photocatalytic degradation activity than Degussa P25 and the undoped or N, S-codoped $TiO_2$ (500 °C) under solar light, indicating that the photocatalytic activity of the P-doped $TiO_2$ (500 °C) nanoparticles has an excellent solar light response. The degradation ratio of RhB over P-doped $TiO_2$ (500 °C) is 90.3% under solar light irradiation after 40 min, 1.3, 3.5 and 4.5 times of those over P25 and the N, S-codoped and undoped $TiO_2$, respectively. Although the N, S-codoped sample had good visible light response [19], its solar-light-sensitive photocatalytic activity is very inferior to herein as-prepared P-doped titania. Additionally, a similar examination was conducted under the UV irradiation to test the degradation efficiency of RhB over P-doped $TiO_2$ (500 °C) (Fig. S4), and the degradation ratio of RhB over P-doped $TiO_2$ (500 °C) is 98.9% under solar light irradiation after 40 min, 1.1 and 2.0 times of those over P25 and undoped $TiO_2$, respectively. Degradation ratio of P-doped under solar light is only a little lower than that under UV light in the same irradiation time, suggesting that such constructed photocatalyst could fully utilize solar light and meet the requirement for practical applications. The high photocatalytic efficiency of the P-doped $TiO_2$ can be attributed to the reconstructed favorable surface structure with the incorporated P–O–Ti bonds and their polyporous structure with high surface area, which is able to facilitate adsorption of water contaminants and effective utilization of UV light in the solar light [29,30,34–36].

The various factors including calcination temperature of photocatalyst, initial concentration of RhB, reuse of the photocatalyst, different catalyst dosage, and different P doping amounts were also systematically investigated to evaluate the P-doped $TiO_2$ photocatalytic degradation efficiency under the solar light irradiation and the obtained results were shown in Fig. 6. It is found that the photocatalytic activity increases up to 500 °C and then decreases with increasing calcination temperatures (Fig. 6a). The P-doped $TiO_2$ calcined at 500 °C owns the highest photocatalytic activity. It can be related to the XRD pictures and BET data. Although the specific surface area P-doped $TiO_2$ calcined at 400 °C is a litter higher than that of the P-doped $TiO_2$ calcined at 500 °C, from the XRD pattern it can be seen that the P-doped $TiO_2$ calcined at 500 °C has better crystallization than P-doped $TiO_2$ calcined at 400 °C. According to the Scherrer equation from the (1 0 1) plane, the average crystallite sizes of P-doped calcined at 400–800 °C is 11.5, 12.1, 13.3, 14.4, 19.3 nm respectively. It was reported that the optimal size of anatase crystal for the excellent photocatalytically active is ~15 nm [40]. Therefore the reason why P-doped $TiO_2$ calcined at 500 °C has the highest photocatalytic activity could be related to its large

**Table 1**
BET surface area of the P-doped (500 °C), undoped $TiO_2$ (500 °C) and P25.

| Catalyst | P-doped $TiO_2$ (500 °C) | Undoped $TiO_2$ (500 °C) | P25 |
|---|---|---|---|
| $S_{BET}$ ($m^2\ g^{-1}$) | 126.93 | 80.53 | 54.54 |

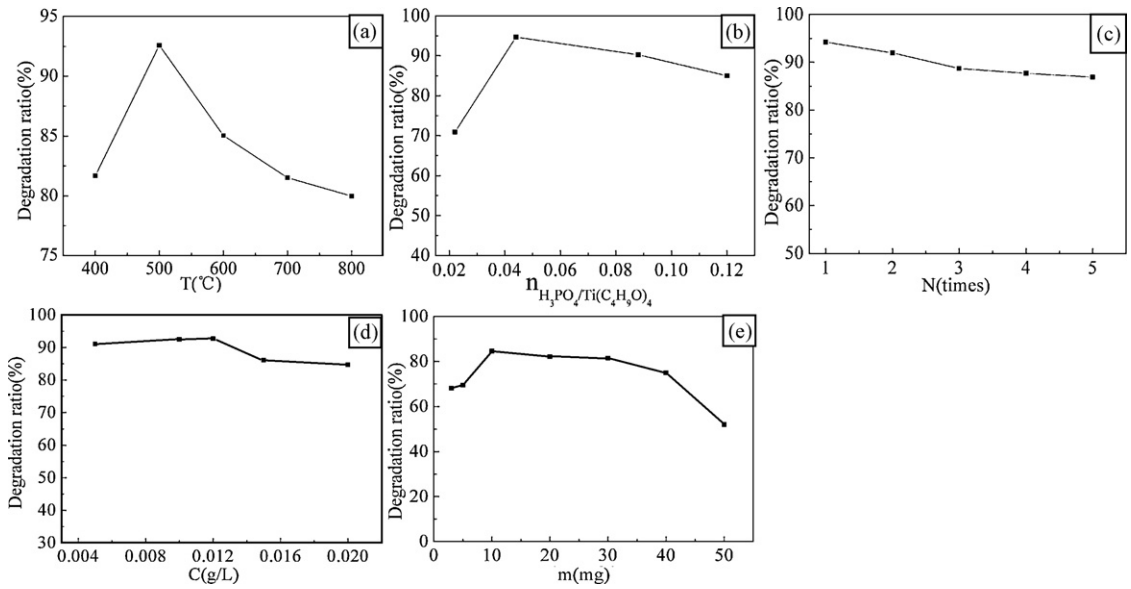


**Fig. 6.** The various factors influencing the photocatalytic activity of P-doped $TiO_2$ under the solar light irradiation: (a) annealing temperature, (b) initial concentration of RhB, (c) reuse of the P-doped $TiO_2$ powders, (d) catalyst loading, and (e) P doping amount.

surface area, good crystallization and appropriate particles size.

Fig. 6b shows the influence of the doping amount of phosphorus on the photocatalytic activity of P-doped $TiO_2$. When the molar ratio of phosphate and tetrabutyl titanate is 0.044, the synthetical sample has the highest photocatalytic activity. At lower contents below the optimum value, $P^{5+}$ could inhibit the recombination between photogenerated electrons and holes by capturing the photogenerated electron with the P content increase in $TiO_2$ [41], leading to enhanced photocatalytic efficiency. However, when the molar ratio exceeded the 0.044, $P^{5+}$ became the recombination center of photogenerated electrons and holes, resulting in a decreased photocatalytic activity [42].

The reuse times are vital to the life of photocatalyst. Fig. 6c shows the influence of the reuse times on the photocatalytic activity of P-doped $TiO_2$. The process of reusing the catalyst is as follows: 5 mg of catalyst powder was added into 3.5 mL of RhB solution (12 mg/L) in a quartz cell and the suspension was sonicated in dark for 10 min before irradiation. After 30 min sunlight irradiation, the suspension was shifted into centrifugal tube and centrifuged. The clear solution above was spilled out and analyzed by recording variations in the absorption in UV–Vis spectra of RhB. The catalyst subsided at the bottom of centrifugal tube was mixed with 3.5 mL of RhB solution (12 mg/L) again, sonicated 10 min under dark, shifted into quartz cell, irradiated 30 min under sunlight and then measured the UV–Vis absorption. As like this, the process was repeated for 4 times. The overall results were shown in Fig. 6c. The first degradation ratio of RhB was 95%, and that of the fifth times was ca. 88%, indicating the P-doped $TiO_2$ had very good stability and could be reused several times without annealing again.

Additionally, the initial RhB concentrations and catalyst loading were also examined on the photocatalytic activity of P-doped $TiO_2$ under the solar light and shown in Fig. 6d and e. It can be seen that the optimal concentration of RhB is 12 mg/L at a given catalyst dosage of 0.2 g/L and the optimal catalyst dosage is 0.4 g/L. The photocatalytic degradation efficiency has been decreased when catalyst dosage is over 0.4 g/L. This could be attributed to shadowing effect, the high turbidity from the high concentration of P-doped $TiO_2$ scatters the solar light, leading to the penetration depth of solar radiation decreased [19,43].

## 4. Conclusions

We have used a conventional sol–gel process to obtain the P-doped titania powder. XRD, UV–Vis absorption spectroscopy, XPS and FTIR showed that the P element has been successfully doped into the titania. The P-doped $TiO_2$ nanoparticles exhibited an enhanced photocatalytic activity for the degradation of rhodamine B as compared with the N, S-codoped and undoped $TiO_2$ and the commercial Degussa P25 under solar light irradiation. Especially the comparable photocatalytic property under solar light irradiation over under UV irradiation endows the P-doped anatase potential in purifying wastewater and meets the requirement for practical applications. Furthermore some factors including calcination temperature of photocatalyst, initial concentration of RhB, reuse of the photocatalyst, different catalyst dosage, and different P doping contents were also systematically investigated to evaluate the P-doped $TiO_2$ photocatalytic degradation efficiency under the solar light irradiation.

## Acknowledgments

This work was financially supported by the Natural Science Foundation of China (Grant No. 20603018) and Science Foundation of Jiangsu (Grant No. BM2007132), as well as China postdoctoral science foundation funded project (20080441029) and Jiangsu planned projects for postdoctoral research funds (0802002C).

## Appendix A. Supplementary data

Supplementary data associated with this article can be found, in the online version, at doi:10.1016/j.jallcom.2009.08.116.

## References

[1] M.R. Hoffman, S.T. Martin, W. Choi, D.W. Bahnemann, Chem. Rev. 95 (1995) 69–96.
[2] A.L. Linsebigler, G. Lu, Y.T. Yates, Chem. Rev. 95 (1995) 735–758.
[3] M.A. Fox, M.T. Dulay, Chem. Rev. 93 (1993) 341–357.
[4] M. Muruganandham, M. Swaminathan, Sol. Energ. Mater. Sol. C 81 (2004) 439–457.

[5] J.C. Yu, J.G. Yu, W.K. Ho, Z.T. Jiang, L.Z. Zhang, Chem. Mater. 14 (2002) 3808–3816.
[6] W. Hoi, A. Termin, M.R. Hoffmann, J. Phys. Chem. 98 (1994) 13669–13679.
[7] G. Colon, M.C. Hidalgo, G. Munuera, I. Ferino, M.G. Cutrufello, J.A. Navio, Appl. Catal. B: Environ. 67 (2006) 41–51.
[8] G. Colon, M.C. Hidalgo, G. Munuera, I. Ferino, M.G. Cutrufello, J.A. Navio, Appl. Catal. B: Environ. 63 (2006) 45–59.
[9] H. Yamashita, Y. Ichihashi, M. Takeuchi, S. Kishiguchi, M. Anpo, J. Synchrotron Rad. 6 (1999) 451–452.
[10] R. Asahi, T. Morikawa, T. Ohwaki, K. Aoki, Y. Taga, Science 293 (2001) 269–271.
[11] S.U.M. Khan, M.A. Shahry, W.B. Ingler, Science 297 (2002) 2243–2245.
[12] J. Cuya, N. Sato, K. Yamamoto, A. Muramatsu, K. Aoki, Y. Taga, Thermochim. Acta 410 (2004) 27–34.
[13] T. Umebayashi, T. Yamaki, H. Itoh, K. Asai, Appl. Phys. Lett. 81 (2002) 454–456.
[14] J.C. Yu, W. Ho, J. Yu, H. Yip, P.K. Wong, J. Zhao, Environ. Sci. Technol. 39 (2005) 1175–1179.
[15] J.A. Rengifo-Herrera, E. Mielczarski, J. Mielczarski, N.C. Castillo, J. Kiwi, C. Pulgarin, Appl. Catal. B: Environ. 84 (2008) 448–456.
[16] Z.P. Wang, W.M. Cai, X.T. Hong, X.L. Zhao, F. Xu, C.G. Cai, Appl. Catal. B: Environ. 57 (2005) 223–231.
[17] J.H. Sun, L.P. Qiao, S.P. Sun, G.L. Wang, J. Hazard. Mater. 155 (2008) 312–319.
[18] K.X. Song, J.H. Zhou, J.C. Bao, Y.Y. Feng, J. Am. Ceram. Soc. 91 (2008) 1369–1371.
[19] Y.Y. Lv, Y. Ding, J.H. Zhou, W.M. Xiao, Y.Y. Feng, J. Am. Ceram. 92 (2009) 938–941.
[20] K. Nagaveni, G. Sivalingam, M.S. Hegde, G. Madras, Appl. Catal. B: Environ. 48 (2004) 83–93.
[21] K. Parida, D.P. Das, J. Photochem. Photobiol. A 163 (2004) 561–567.
[22] Q. Shi, D. Yang, Z. Jiang, J. Li, J. Mol. Catal. B 43 (2006) 44–48.
[23] K.J. Antony Raj, A.V. Ramaswamy, B. Viswanathan, J. Phys. Chem. C 113 (2009) 13750–13757.
[24] H. Ozaki, N. Fujimoto, S. Iwamoto, M. Inoue, Appl. Catal. B: Environ. 70 (2007) 431–436.
[25] L. Lin, W. Lin, Y.X. Zhu, B.Y. Zhao, Y.C. Xie, Chem. Lett. 34 (2005) 284–285.
[26] L. Lin, W. Lin, J.L. Xie, Y.X. Zhu, B.Y. Zhao, Y.C. Xie, Appl. Catal. B: Environ. 75 (2007) 52–58.
[27] L. Lin, R.Y. Zheng, J.L. Xie, Y.X. Zhu, Y.C. Xie, Appl. Catal. B: Environ. 76 (2007) 196–202.
[28] J.C. Yu, L. Zhang, Z. Zheng, J. Zhao, Chem. Mater. 15 (2003) 2280–2286.
[29] R.Y. Zheng, L. Lin, J.L. Xie, Y.X. Zhu, Y.C. Xie, J. Phys. Chem. C 112 (2008) 15502–15509.
[30] K.S. Yang, Y. Dai, B.B. Huang, J. Phys. Chem. C 111 (2007) 18985–18994.
[31] Y.Y. Lv, L.S. Yu, H.Y. Huang, H.L. Liu, Y.Y. Feng, Appl. Surf. Sci. 255 (2009) 9548–9552.
[32] J. Lin, Y. Lin, P. Liu, M.J. Meziani, L.F. Allard, Y.P. Sun, J. Am. Chem. Soc. 124 (2002) 11514–11518.
[33] Q. Shi, D. Yang, Z.Y. Jiang, J. Li, J. Mol. Catal. B: Enzymat. 43 (2006) 44.
[34] G. Liu, Y.N. Zhao, C.H. Sun, F. Li, G.Q. Lu, H.M. Cheng, Angew. Chem. Int. Ed. 47 (2008) 4516–4520.
[35] G. Liu, C.H. Sun, X.X. Yan, L.N. Cheng, Z.G. Chen, X.W. Wang, L.Z. Wang, S.C. Smith, G.Q. Lu, H.-M. Cheng, J. Mater. Chem. 19 (2009) 2822–2829.
[36] G. Liu, C.H. Sun, L.N. Cheng, Y.G. Jin, H.F. Lu, L.Z. Wang, S.C. Smith, G.Q. Lu, H.-M. Cheng, J. Phys. Chem. C 113 (2009) 12317–12324.
[37] O. Legrini, E. Oliveros, A.M. Braun, Chem. Rev. 93 (1993) 671–698.
[38] D. Ollis, F.H. Al-Ekabi (Eds.), Photocatalytic Purification and Treatment of Water and Air, Elsevier Science Publishers, Amsterdam, 1993.
[39] C.S. Turchi, D.F. Ollis, J. Catal. 122 (1990) 178–192.
[40] P. Periyat, S.C. Pillai, D.E. McCormack, J. Colreavy, S.J. Hinder, J. Phys. Chem. C 112 (2008) 7644–7652.
[41] M.D. Ward, A.J. Bard, J. Phys. Chem. 86 (1982) 3599–3605.
[42] J.W. Pavlik, S.W. Tantayanon, J. Am. Chem. Soc. 103 (1981) 6755–6757.
[43] Q. Xiao, J. Zhang, C. Xiao, Z.C. Si, X.K. Tan, Sol. Energy 82 (2008) 706–713.